Pergamon

Geochimica et Cosmochimica Acta, Vol. 66, No. 21, pp. 3719–3732, 2002

0016-7037/02 $22.00 + .00

PII S0016-7037(01)00900-0

Gold solubility, speciation, and partitioning as a function of HCl in the brine-silicate melt-metallic gold system at 800°C and 100 MPa

MARK R. FRANK,[1,†] PHILIP A. CANDELA,[1] PHILIP M. PICCOLI,[1] and MICHAEL D. GLASCOCK[2]

[1]Laboratory for Mineral Deposits Research, Department of Geology, University of Maryland, College Park, MD 20742, USA
[2]Research Reactor Center, University of Missouri, Columbia, MO 65211, USA

(*Received October* 6, 2001; *accepted in revised form December* 10, 2001)

Abstract—A vapor-undersaturated synthetic brine was equilibrated with metallic gold and a haplogranitic melt at 800°C and 100 MPa to examine the solubility, speciation and partitioning of gold in the silicate melt-brine-metallic gold system. The starting composition of the NaCl-KCl-HCl-H_2O brine was 70 wt.% NaCl (equivalent) with starting KCl/NaCl ranging from 0.5 to 1. KCl/HCl was varied from 3.2 to 104 to evaluate the solubility and partitioning of gold as a function of the concentration of HCl in the brine. Inclusions of brine were trapped in a silicate glass during quench. Inclusion-poor and inclusion-rich portions of glass were analyzed for gold and chloride by using neutron activation analysis. The inclusion-poor glass yielded an estimate of the solubility of gold and chloride in the silicate melt. The solubility of gold in the melt, at gold metal saturation, was estimated as ≈1 ppm. The solubility of gold in the brine was estimated by mass balance, given the concentration of gold and chloride in the inclusion-poor and inclusion-rich glasses. The solubility of gold metal at low-HCl concentrations in the brine, C^b_{HCl}, (3×10^3 to 1.1×10^4 ppm) is ≈40 ppm (by weight) and is independent of the HCl concentration under those conditions. For C^b_{HCl} of 1.1×10^4 to 4.0×10^4 ppm, the solubility of gold increased from 40 to 840 ppm, and the solubility is given by:

$$\log C^b_{Au} = [2.2 \cdot \log C^b_{HCl}] - 7.2 \quad (1)$$

These data suggest that a significant amount of gold is not chloride complexed in brines at low-HCl concentrations ($< 1.1 \times 10^4$ ppm), but that gold-chloride complexes, possibly $AuCl_2H$, are important at elevated concentrations of HCl ($> 1.1 \times 10^4$ ppm). The calculated Nernst partition coefficient ($D^{b/m}_{Au}$) for gold between a brine and melt varied from 40 to 830 over a range of brine HCl concentrations of 3×10^3 to 1.1×10^4 ppm. Our results indicate a significant amount of gold can be transported by a brine in the magmatic-hydrothermal environment independent of the fugacity of sulfur in the system. Thus brines provide an effective mechanism for the scavenging of gold from a crystallizing melt and transport into an associated magmatic-hydrothermal system, regardless of their sulfur contents. *Copyright © 2002 Elsevier Science Ltd*

1. INTRODUCTION

Magmatic-hydrothermal gold deposits account for ~20% of all gold deposits (Singer, 1995). Porphyry gold and gold-bearing porphyry copper deposits are associated spatially and temporally with porphyritic granitic (i.e., diorite to granite, s.s.) intrusions (Sillitoe, 1979, 1989) and account for 10% of world gold production (Singer, 1995). A confluence of structural, fluid inclusion, isotopic, and experimental evidence suggests that the formation of porphyry-type deposits involve the partitioning of ore metals into an exsolving magmatic volatile phase (Holland, 1972; Burnham, 1979; Candela and Holland, 1984; Heinrich et al., 1992; Gammons and Williams-Jones, 1997). However, most experimental studies on gold solubility and speciation have concentrated on lower temperature hydrothermal environments representative of epithermal regimes (Pan and Wood, 1991; Benning and Seward, 1996; Gibert et al., 1998). While the genetic relationship between the epithermal and porphyry environments has been demonstrated in a few select cases (Richards et al., 1991; Richards and Kerrich, 1993; Richards and Ledlie, 1993; Hedenquist et al., 1998), few constraints have been placed on the source of gold in these systems. Owing to the dearth of experimental data on gold at near magmatic conditions, some studies have concluded, based in part on the observed strong chloride complexation of copper, that gold may concentrate in the high-salinity aqueous phase (Gammons and Williams-Jones, 1997). However, Loucks and Mavrogenes (1999) found high concentrations of gold in a sulfidic aqueous solution over a wide range of temperature (550–725°C) and pressure (110–400 MPa). They concluded that gold was sulfide-complexed in a pyrite-saturated aqueous solution and was insensitive to changes in pH at geologically reasonable conditions. Loucks and Mavrogenes (1999) suggest that the major gold species under the condition of their experiments was $AuHS(H_2S)_3$. Their reconnaissance experiments attempted to evaluate gold solubility under conditions of gold deposition in equilibrium with mineral pH buffers. However, it is clear from studies such as those of Williams et al. (1997), Piccoli et al. (1999), and Frank et al. (1998) that the concentrations of HCl in the magmatic volatile phase during ore transport can be significantly different from those that prevail after neutralization and deposition. Based on the occurrence of gold in porphyry-type deposits, we attempt herein to determine the conditions of gold transport in sulfur-free brines, as a prelude to studies of more complex, sulfur-bearing, vapor-brine systems. Important terms and variables are listed in Table 1.

* Author to whom correspondence should be addressed (m.frank@gl.ciw.edu).
† *Present address:* Geophysical Laboratory, Carnegie Institution of Washington, Washington, D.C. 20015, USA.

Table 1. Teminology, variables, and notations.

	Terminology
Brine:	high-salinity liquid phase
MVP:	(magmatic volatile phase) refers to any gas or aqueous chloride-bearing liquid which exsolves from a silicate melt
Melt:	silicate melt
	Variables
C_i^x:	concentration of component i in phase x
mf_x:	mass fraction of phase x in phase mixture x + y
$D_i^{x/y}$:	Nernst-type partition coefficient for component i between phases x and y
a_i^x:	activity of component i in phase x ($a_i^x = \gamma_i^x \cdot C_i^x$)
γ_i^x:	activity coefficient of component i in phase x
f_i^x:	fugacity of component i in phase x
K_h (T,P):	equilibrium constant of equilibrium h at a given temperature and pressure
K'_h (T,P):	apparent equilibrium constant of equilibrium h at a given temperature and pressure (does not account for activity coefficients)
	Notation
aq	aqueous phase (vapor, brine, or supercritical fluid)
b	brine
v	vapor
m	melt
g+b	phase mixture (glass + brine)

2. EXPERIMENTAL AND ANALYTICAL METHODS

2.1. Experimental Procedures

A brine (b) was equilibrated with a silicate melt (m) and metallic gold at 800°C and 100 MPa at a constant oxygen fugacity (Ni-NiO; a summary of experimental conditions is listed in Table 2 and Fig. 1). Experiments were conducted in gold capsules (the source of gold in the experiments) with an outer diameter of 5.0 mm, inner diameter of 4.8 mm, and length of ~20 mm. Approximately 50 mg of powdered glass (Table 2) and brine-starting materials were loaded into each capsule (Fig. 1). The glass, $Qtz_{0.38}Ab_{0.33}Or_{0.29}$ on an anhydrous basis, had the composition of a 100 MPa minimum melt (with a solidus temperature of ~710°C). The initial porosity of the glass powder in the experiments was varied by modifying the mechanical compression of the starting glass; in that way, alterable volumes of fluid were trapped during the run and preserved as inclusions in each quenched glass sample. Brines were prepared so that the total chloride concentration corresponded to the subcritical, "liquid only" phase stability field in the NaCl-H_2O system (determined by using the data of Sourirajan and Kennedy, 1962; Bodnar et al., 1985; Chou et al., 1992; Sterner et al., 1992; Anderko and Pitzer, 1993). The system NaCl-H_2O was used to provide a reasonable first-order approximation of the colligative properties of our NaCl-KCl-HCl-H_2O solution. Capsules were crimped, weighed, and sealed using a carbon electrode arc welder. During the closure weld, the capsules were chilled with dry ice to minimize vaporization of the volatile components.

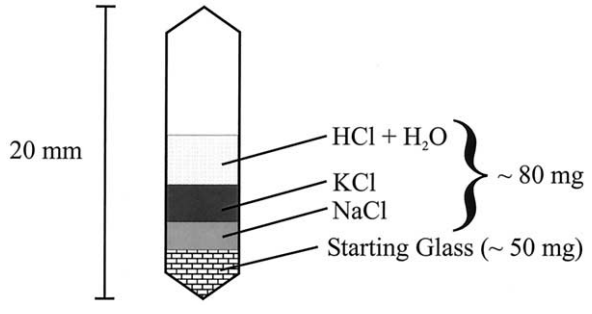

Fig. 1. Schematic representation of the capsule technique used in this study. Tightly packed glass starting material would produce a quenched glass with fewer fluid inclusions than finely powdered glass starting material, allowing us to generate glass samples with variable proportions of fluid inclusions.

Experiments were conducted in cold-seal pressure vessels. The vessels (René 41, an Ni-based alloy) were heated externally by means of alumina tube furnaces fitted with Kanthal windings. The furnaces were doubly wound, minimizing thermal gradients across the capsule, and inclined at a 12° angle to minimize convection at the hot end of the vessel. Temperatures were measured with type K (Chromel-Alumel) external thermocouples positioned close to the midpoint of the capsule. External thermocouple readings were calibrated against readings from internal thermocouples under run conditions and found to be within ± 2°C. The position of the internal thermocouple was varied to determine the gradient across the length of the capsule (± 3°C). Pressure was regulated by a pressure intensifier with water as the pressure medium and monitored with Bourdon-tube gauges (± 2 MPa), which were calibrated against a factory-calibrated Heise gauge.

Oxygen fugacity was controlled by the pressure medium or by the use of a solid-state buffer (Ni-NiO). The oxygen fugacities of the vessels were measured, with no internal Ni-NiO buffer, by using the hydrogen fugacity sensor technique (HCl-AgCl; H_2O-AgCl), as described by Chou (1987), and yielded a log oxygen fugacity of -14.0 ± 0.1 (log oxygen fugacity at Ni-NiO = −13.9) at 800°C and 100 MPa. To investigate the diffusion of H_2 through gold, and thus the effectiveness of the Ni-NiO buffer, two gold capsules were run side by side in a René 41 vessel with an Ni-NiO buffer. One gold capsule contained Ni only, and the other NiO only. The experiments were run for 6 days at 800°C and 100 MPa. Each capsule contained Ni and NiO after the experiment, demonstrating significant diffusion of H_2 through the gold capsule within the 6-day duration of the experiment.

Experiments were quenched isobarically by removing the vessel from the furnace and placing it in a stream of compressed air while open to a large reservoir pressure buffer set to 100 MPa. This method cooled the vessel to < 300°C in ~1 min. The vessel was then placed in a reservoir of water to complete the quench to room temperature. The total quench time was ~2 min. The capsules were removed from the vessels, cleaned, and weighed to check for any leakage during the experiments. Any capsule exhibiting a weight loss ≥ 0.3 mg at any point of the experimental procedure was discarded.

2.2. Analytical Procedures

Glass fragments were inspected using a petrographic microscope to examine fluid inclusions contained within the glass. The fragments were separated, based on the qualitative number of inclusions, into inclusion-poor and inclusion-rich categories. Samples were also inspected using a binocular microscope to check the surface of the glass fragments for any gold that may have adhered to the surface.

Analyses of major elements (Si, Al, K, Na, Ca, Fe, and Cl) in glass-run products were accomplished using a JEOL 8900 electron microprobe. Samples were prepared for analysis by coating them with ~300 Å of carbon by standard thermal evaporation techniques. Analyses were performed at 15 kV and 5 nA with minimum counting times of 20 s (sum of peak and background). Each glass was analyzed at 10 points to evaluate homogeneity. X-ray intensities for each element were corrected using a primary and secondary standard (primary = Yellowstone Rhyolite [NMNH 72854 VG568] and secondary = Tulancingo Rhyolite [USGS RLS 132]). The composition of the starting materials was compared to those of the run products to calculate the mass transfer of cations that may have occurred during the experiments.

Analyses for gold and chloride were conducted by using neutron activation (conducted at the University of Missouri Research Reactor). Glass fragments were placed in a microvacuum funnel and soaked in aqua regia (3 parts concentrated HCl and 1 part concentrated HNO_3, by

Table 2. Summary of experimental conditions.

Run	Duration (hours)	Temperature (°C)	KCl/NaCl (mole)	KCl/HCl (mole)	Log f_{O_2} (bars)
1	475.0	800 ± 3	1.00 ± 0.01	104 ± 2	−14.0 ± 0.1
2	359.8	800 ± 3	1.00 ± 0.01	104 ± 2	−14.0 ± 0.1
3	512.2	796 ± 5	1.00 ± 0.01	104 ± 2	−14.0 ± 0.1
4	742.8	796 ± 5	1.00 ± 0.01	104 ± 2	−14.0 ± 0.1
5	742.9	800 ± 3	1.00 ± 0.01	104 ± 2	−14.0 ± 0.1
6	453.2	796 ± 5	1.00 ± 0.01	104 ± 2	−14.0 ± 0.1
7	1127.0	800 ± 3	1.00 ± 0.01	104 ± 2	−14.0 ± 0.1
8	885.5	800 ± 3	1.00 ± 0.01	104 ± 2	−14.0 ± 0.1
9	885.0	800 ± 3	1.00 ± 0.01	104 ± 2	−14.0 ± 0.1
10	146.0	800 ± 3	1.00 ± 0.01	750 ± 8	−14.0 ± 0.1
11	232.0	800 ± 3	1.00 ± 0.02	10.9 ± 0.1	−14.0 ± 0.1
12	581.7	800 ± 3	1.00 ± 0.02	10.9 ± 0.1	−14.0 ± 0.1
13	308.3	800 ± 3	1.00 ± 0.02	10.9 ± 0.1	−14.0 ± 0.1
14	383.0	800 ± 3	1.00 ± 0.02	10.9 ± 0.1	−14.0 ± 0.1
15	329.0	800 ± 3	1.00 ± 0.02	10.9 ± 0.1	−14.0 ± 0.1
16	208.2	800 ± 3	1.00 ± 0.02	10.9 ± 0.1	−14.0 ± 0.1
17	287.3	800 ± 3	1.00 ± 0.02	10.9 ± 0.1	−14.0 ± 0.1
18	520.2	800 ± 3	1.00 ± 0.02	5.30 ± 0.08	−14.0 ± 0.1
19	278.5	800 ± 3	1.00 ± 0.02	5.30 ± 0.08	−14.0 ± 0.1
20	307.5	800 ± 3	1.00 ± 0.02	5.30 ± 0.08	−14.0 ± 0.1
21	92.7	800 ± 3	1.00 ± 0.02	5.17 ± 0.07	−14.0 ± 0.1
22	669.2	800 ± 3	1.00 ± 0.02	5.17 ± 0.07	−14.0 ± 0.1
23	756.5	800 ± 3	1.00 ± 0.02	5.17 ± 0.07	−14.0 ± 0.1
24	140.0	798 ± 4	0.500 ± 0.004	3.20 ± 0.04	−14.0 ± 0.1

All experiments were performed at 100 ± 2 MPa and log f_{O_2} (bars) = −14.0 ± 0.1 with a 70.0 ± 0.2 wt. NaCl (eq.) brine. The KCl/NaCl and KCl/HCl values listed above are representative of the starting composition of the brine and are not equilibrium values. Brine compositions (KCl/NaCl and KCl/HCl) would be modified by exchange reactions with the melt. Durations represent the elapsed times of the experiments from the time when the experiments reached thermal equilibrium to quench. Uncertainty in run duration is ± 0.1 hours. We varied the durations of the experiments to demonstrate equilibrium with respect to time (i.e., no change in gold solubility and partitioning as a function of time).

volume) for 5 min to remove any gold adhering to the surface of the glass fragments and then rinsed with doubly deionized and distilled H_2O. Each sample was soaked in doubly deionized and distilled H_2O for 10 min to remove residual aqua regia and then washed for an additional 10 min.

Samples and three standards each for chloride and gold were placed in high-density polyethylene vials and irradiated for 30 s in a neutron flux of 8×10^{13} n × cm^{-2} × sec^{-1}. Samples were allowed to decay for 25 min to allow for a reduction in short-lived activity (due to, e.g., ^{28}Al); samples were counted for 12 min at a distance of 10 cm from the face of a hyperpure germanium (HPGe) detector to measure ^{38}Cl (half-life of 37.2 min) at the 2168-keV gamma ray. Counting for ^{198}Au was conducted for 60 min 18 to 24 h after irradiation at the 412-keV gamma ray. All samples were rotated during counting to reduce any uncertainty associated with variable sample size and shape (Glascock, 1998).

Analyses for gold and chloride in the quenched glasses were also conducted by using Secondary Ion Mass Spectrometry (SIMS; analyses performed by Richard Hervig at Arizona State University). By analyzing the glass for gold and chloride, the SIMS method provided a means to discriminate the gold contained in the silicate glass from the gold included within the fluid inclusions. INAA analyses of the glass + brine phase mixture cannot separate independently the gold in fluid inclusions from the gold in the glass. Therefore, using chloride in the analyses allowed for the influence of gold contained within a fluid inclusion to be detected in the analyses of the glass-only component of the glass + brine phase mixture.

Analyses were conducted using the negative secondary ions and a K primary beam to bombard the sample (McMahon et al., 2000). A normal incidence electron gun was used to alleviate charge, and three NIST glass standards (NIST 610, 612, and 614) were used to calibrate the signal. A regression of the data for the glass standards, forcing the result through the origin, gave a linear regression with a slope of 1.004×10^{-4} and $r^2 = 0.990$. Sample analyses were obtained by sputtering a crater on the sample and collecting ion intensities for ^{18}O, ^{30}Si, ^{35}Cl, and ^{197}Au (all negative ions). All ion signals were integrated for 5 s during each cycle, with the total number of cycles ranging from 30 to 82, depending on the sample. This spanned an actual analysis time of ~15 to 30 min. Counting statistics indicate that the relative error on each cycle was at least 20% (and often much more on low Au areas), whereas the integrated Au signal indicated a counting error ranging from 20% on the lowest Au sample to ~2% on the highest gold sample.

3. RESULTS

3.1. Petrographic Characterization of Glass-Run Products

Glass samples were characterized qualitatively based on the number of fluid inclusions trapped within the glass. Fluid inclusions of brine were trapped in the melt/glass as the melt was cooled through the glass transition state and contained (1) a vapor bubble, (2) liquid, and (3) multiple halite/sylvite crystals. Glass samples with a low initial porosity would typically, but not always, produce a glass with fewer fluid inclusions (Fig. 2a) than a glass with high initial porosity (Fig. 2b,c). The consistent production of fluid inclusion-poor glasses proved problematic. The brine interacted intimately with the melt and produced a large number of fluid inclusions once the melt was quenched to a glass. Reducing the initial porosity of the glass loaded in the experiment reduced the number of fluid inclusions, but the glasses could still contain 2 to 3% (mass) fluid inclusions. Decreasing the ratio of fluid to melt in the experi-

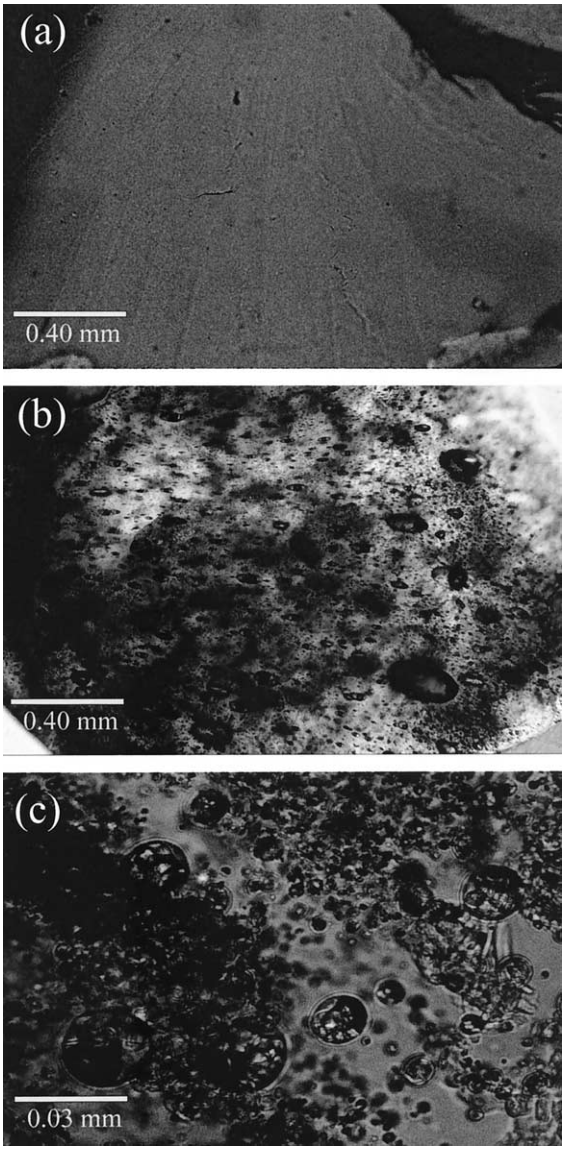

Fig. 2. (a) Photograph of a quenched glass-run product with few visible fluid inclusions. The starting glass was tightly packed and yielded a quenched glass with few fluid inclusions. Long dimension of the photograph is 2.0 mm. (b) Photograph of a quenched glass-run product with many fluid inclusions. The starting glass was finely powdered and trapped a large number of fluid inclusions on quenching. Long dimension of the photograph is 2.0 mm. (c) Photograph of quenched run product illustrating the density of fluid inclusion. Large fluid inclusions containing daughter crystals (NaCl + KCl), liquid, and vapor are representative of the composition of the brine at equilibrium in the metallic gold-brine-silicate melt system. Long dimension of the photograph is 0.15 mm.

ment also reduced the number of fluid inclusions trapped, but a relatively large mass of fluid was required in the experiment to insure that the fluid composition did not change drastically during the run. Preliminary experiments in the melt-vapor-gold system indicate that a fluid inclusion-poor glass is more easily produced in this system. Few crystals were observed in the glass samples, indicating that the glasses were quenched from a nearly aphyric melt and that the quench was fast enough to prevent crystal growth, which could produce local heterogeneities that cause variations in the concentrations of gold in the glass beads.

Table 3. Starting chemical composition of the glass, minimum melt composition at 100 MPa; LOI = loss on ignition, analysis performed by Activation Laboratories by XRF.

Oxide	Weight Percent (as oxide)
Na_2O	3.67
K_2O	4.43
CaO	0.17
Fe_2O_3	0.04
Al_2O_3	11.09
SiO_2	75.18
TiO_2	0.03
MnO	0.01
MgO	0.10
P_2O_5	0.03
LOI	4.51
Total	99.26

3.2. Melt Composition: Major and Minor Elements

The composition of the melt in each experiment was altered systematically due to interaction with the brine. The melt became enriched in potassium and chloride and depleted in sodium relative to the starting glass (refer to Table 3 and Table 4). Higher concentrations of HCl in the starting brine resulted in greater enrichment of potassium and chloride and greater depletion of sodium in the melt. The enrichment of potassium in the melt was of greater magnitude than the depletion of sodium and calcium, resulting in an enrichment of alkalis in the melt relative to aluminum at low HCl concentrations. High HCl concentrations in the brine effectively stripped alkalis from the melt relative to aluminum.

Melt aluminosity is described using the aluminum saturation index (ASI) as defined by Shand (1951), with ASI = [molar: $Al_2O_3/(CaO + K_2O + Na_2O)] > 1.0$, corresponding to an excess of aluminum in the melt relative to alkalis. The starting glass had an ASI of 1.0. Melt aluminosity has been shown to be of major importance in controlling the chemistry of an MVP, with a highly aluminous melt producing an MVP with a high HCl concentration (Candela, 1990; Candela and Piccoli, 1995; Williams et al., 1997). Low HCl ($n = 8$) and moderate to high-HCl ($n = 15$) glass-run products have a mean ASI value of 0.93 ± 0.03 (1σ) and 0.99 ± 0.04 (1σ), respectively, which is broadly consistent with the theoretical model of Candela (1990).

The concentration of chloride in a silicate melt is controlled, in part, by the concentration of chloride in a coexisting aqueous fluid. To date, the chloride species present in a silicate melt are not well known. We hypothesize here for our synthetic system that a majority of chloride in the melt is complexed as NaCl and KCl. Thus increased chloride concentration in the melt will also increase the concentration of sodium and potassium, which is not bound in the feldspar-like structure. The calculated values of ASI are not comparable with low-chloride systems because a portion of alkalis was not associated with aluminum. Therefore, it may be more appropriate to use a modified version of Shand's ASI calculation to compare low- and high-chloride

Table 4. Analyses of major elements for glass run products in wt.%.

Run	Na_2O	K_2O	CaO	FeO	Al_2O_3	SiO_2	Cl	Total
1	2.70 ± 0.09	6.45 ± 0.15	0.05 ± 0.01	0.17 ± 0.06	10.77 ± 0.22	76.22 ± 0.45	0.18 ± 0.01	96.54
2	2.76 ± 0.08	5.97 ± 0.06	0.03 ± 0.02	0.26 ± 0.04	10.75 ± 0.20	75.33 ± 0.35	0.16 ± 0.02	95.26
3	2.77 ± 0.14	6.47 ± 0.21	0.08 ± 0.04	0.07 ± 0.04	11.05 ± 0.28	74.1 ± 0.6	0.24 ± 0.02	94.80
4	2.69 ± 0.08	6.40 ± 0.10	0.04 ± 0.02	0.10 ± 0.05	11.15 ± 0.24	75.7 ± 0.6	0.22 ± 0.02	96.28
5	2.79 ± 0.12	6.42 ± 0.14	bd	bd	11.04 ± 0.25	75.00 ± 0.33	0.20 ± 0.01	95.45
6	2.71 ± 0.06	6.05 ± 0.06	bd	0.04 ± 0.02	10.88 ± 0.12	75.69 ± 0.33	0.16 ± 0.02	95.53
7	2.58 ± 0.04	6.49 ± 0.08	bd	bd	10.70 ± 0.16	75.46 ± 0.48	0.22 ± 0.02	95.45
8	2.88 ± 0.19	6.17 ± 0.10	bd	bd	10.80 ± 0.15	75.26 ± 0.40	0.17 ± 0.01	95.28
9	2.46 ± 0.08	6.10 ± 0.06	0.04 ± 0.02	0.18 ± 0.06	10.75 ± 0.14	75.74 ± 0.17	0.18 ± 0.02	95.45
10	3.44 ± 0.31	4.94 ± 0.24	0.04 ± 0.02	0.08 ± 0.02	10.7 ± 0.8	77.1 ± 0.9	0.07 ± 0.01	96.40
11	1.97 ± 0.12	6.41 ± 0.24	0.13 ± 0.05	0.11 ± 0.04	10.18 ± 0.43	73.1 ± 0.8	0.21 ± 0.01	92.11
12	1.90 ± 0.21	6.90 ± 0.09	bd	0.02 ± 0.01	11.18 ± 0.18	74.46 ± 0.40	0.21 ± 0.01	94.67
13	1.82 ± 0.22	6.92 ± 0.15	0.01 ± 0.01	0.05 ± 0.02	11.45 ± 0.45	73.7 ± 0.6	0.26 ± 0.02	94.25
14	1.96 ± 0.22	6.64 ± 0.13	0.03 ± 0.02	0.03 ± 0.02	10.56 ± 0.17	75.38 ± 0.45	0.18 ± 0.01	94.78
15	1.68 ± 0.18	6.95 ± 0.12	0.04 ± 0.02	bd	10.78 ± 0.48	74.2 ± 0.8	0.27 ± 0.03	93.88
16	2.13 ± 0.28	6.70 ± 0.12	0.05 ± 0.02	0.05 ± 0.02	10.64 ± 0.22	75.68 ± 0.37	0.20 ± 0.01	95.45
17	1.89 ± 0.13	6.92 ± 0.15	0.04 ± 0.02	0.06 ± 0.03	10.52 ± 0.35	74.79 ± 0.45	0.24 ± 0.02	94.46
18	2.43 ± 0.22	6.51 ± 0.13	0.16 ± 0.05	0.07 ± 0.03	10.24 ± 0.11	72.51 ± 0.38	0.22 ± 0.02	92.14
19	2.37 ± 0.08	6.83 ± 0.09	0.08 ± 0.02	0.06 ± 0.03	10.88 ± 0.07	73.0 ± 0.7	0.26 ± 0.02	93.49
20	2.16 ± 0.16	6.38 ± 0.13	0.04 ± 0.02	0.04 ± 0.02	10.67 ± 0.26	73.55 ± 0.48	0.24 ± 0.01	93.08
21	1.97 ± 0.06	6.78 ± 0.08	0.01 ± 0.01	0.06 ± 0.03	10.57 ± 0.24	75.1 ± 0.5	0.25 ± 0.02	94.78
22	1.99 ± 0.16	6.92 ± 0.18	0.04 ± 0.02	0.04 ± 0.02	10.71 ± 0.21	75.64 ± 0.49	0.20 ± 0.01	95.54
23	2.08 ± 0.13	6.40 ± 0.25	bd	bd	10.35 ± 0.33	76.0 ± 0.9	0.29 ± 0.02	95.16
24	3.44 ± 0.20	5.36 ± 0.12	0.05 ± 0.02	0.03 ± 0.01	10.75 ± 0.23	76.10 ± 0.44	0.28 ± 0.06	96.01

Each glass was analyzed in 10 separate areas of the sample to evaluate glass homogeneity. X-ray intensities for each element were corrected using two standards (Yellowstone Rhyolite and Tulancingo Rhyolite). Uncertainties are presented as the standard deviation from the mean (1σ) for the 10 measurements of each glass.

systems. Sodium and potassium bound to chloride can be accounted for using ASI* = (molar: $[Al_2O_3/(CaO + K_2O + Na_2O - Cl)]$) (Table 4).

3.3. Instrumental Neutron Activation Analysis: Gold and Chloride

3.3.1. Phase mixtures (melt + brine)

Glass samples, both fluid inclusion-poor and inclusion-rich, contain very low concentrations of gold, and thus, Instrumental Neutron Activation Analysis (INAA) was employed to determine the gold and chloride concentrations in the phase mixtures (Table 5; Fig. 3). The influence of the HCl concentration of the brine on gold concentration in the brine + melt phase mixture can be seen in Figure 3. A glass with few fluid inclusions has gold and chloride concentrations that approach those of the single-phase silicate melt, whereas a glass with many trapped brine inclusions will cause the phase mixture to be elevated in gold and chloride relative to a silicate melt. The glass starting material was powdered, so a large number of fluid inclusions were trapped in each experiment; the mass fraction of brine in the quenched glass + brine phase mixture (mf_b) ranged from 2.9 to 4.9%. mf_b was calculated for each glass by relating the chloride concentrations of the brine (this was kept near constant by using a high brine to melt ratio in the experiments) and glass (through EPMA analyses) to the chloride analyses of the glass + brine phase mixture (INAA).

3.3.2. Gold solubility in silicate glasses

In previous studies in sulfur-free and sulfur-bearing assemblages (Candela et al., 1996; Jugo et al., 1999), preliminary data indicated the solubility of gold in silicate melts in equilibrium with high-HCl vapors was on the order of 2 to 4 ppm (by weight). The independence of gold solubility as a function of sulfur, within the uncertainty in the data, suggests that Au-S species do not predominate in silicate melts. Data from this study demonstrate, for the runs with the lowest HCl concentrations in the brine, that the concentrations of gold and chloride in the glass + brine phase mixtures are on the order of 2 ppm and 2 wt.%, respectively, whereas chloride concentrations of the glasses, as determined by using EPMA, are 0.06 to 0.23 wt.%. These data are consistent with petrographic observations that a significant number of fluid inclusions are present in the glasses, suggesting that the gold concentrations in the glasses are significantly below 2 ppm. Experiments performed at higher HCl concentrations produced glass + brine mixtures that were elevated in gold relative to glasses from lower HCl experiments (see Fig. 3 for reference). The variable entrapment of fluid inclusions in each glass sample was used to calculate the concentration of gold in a glass devoid of fluid inclusions by extrapolating to a fluid inclusion free glass (mass fraction of brine in the glass + brine phase mixture, mf_b, = 0), allowing for the estimation of the solubility of gold in a silicate melt at the conditions of the experiments. To limit the influence of the higher HCl experiments on the extrapolated concentration of gold in the glass, only experiments that had equilibrium HCl concentrations of $< 1.41 \times 10^4$ ppm were used in the extrapolation. These experiments have gold concentrations for the glass + brine mixtures that fall along a line that has a slope close to zero relative to HCl, indicating little influence by HCl in the brines on the concentration of gold in the glass + brine phase mixtures. Regression analyses of the five experiments with brine HCl concentrations $> 4.2 \times 10^3$ and $< 1.4 \times 10^4$

Table 5. Results (all ppm values are by weight) of Au and Cl analyses for each phase mixtures of glass + brine (Au_{g+b} and Cl_{g+b}, respectively) were completed by using INAA.

Run	Au_{g+b} (pmm) [INAA]	Cl_{g+b} (ppm) [INAA]	Cl_g ppm [EPMA]	mf_b	HCl_b (ppm)
Starting KCl/HCl ≈ 100					
1	2.1 ± 0.7	$1.82 \pm 0.01 \cdot 10^4$	$1.8 (\pm 0.2) \cdot 10^3$	0.039	$3.7 (\pm 0.4) \cdot 10^3$
2	3.1 ± 0.8	$1.70 \pm 0.01 \cdot 10^4$	$1.6 (\pm 0.4) \cdot 10^3$	0.037	$5 (\pm 1) \cdot 10^3$
3	2.6 ± 0.7	$1.96 \pm 0.01 \cdot 10^4$	$2.4 (\pm 0.4) \cdot 10^3$	0.039	$2.4 (\pm 0.3) \cdot 10^3$
4	3.3 ± 0.6	$2.09 \pm 0.01 \cdot 10^4$	$2.2 (\pm 0.5) \cdot 10^3$	0.044	$2.3 (\pm 0.5) \cdot 10^3$
5	3.3 ± 0.6	$1.94 \pm 0.01 \cdot 10^4$	$2.0 (\pm 0.2) \cdot 10^3$	0.041	$0.9 (\pm 0.5) \cdot 10^3$
6	2.3 ± 0.6	$1.88 \pm 0.01 \cdot 10^4$	$1.6 (\pm 0.3) \cdot 10^3$	0.041	$4 (\pm 1) \cdot 10^3$
7	2.3 ± 0.5	$2.04 \pm 0.01 \cdot 10^4$	$2.2 (\pm 0.5) \cdot 10^3$	0.043	$8.2 (\pm 0.8) \cdot 10^3$
8	2.1 ± 0.7	$1.95 \pm 0.01 \cdot 10^4$	$1.7 (\pm 0.1) \cdot 10^3$	0.037	$0.9 (\pm 0.3) \cdot 10^3$
9	2.8 ± 0.7	$2.07 \pm 0.01 \cdot 10^4$	$1.8 (\pm 0.1) \cdot 10^3$	0.044	$1.0 (\pm 0.4) \cdot 10^3$
10	2.0 ± 0.6	$1.75 \pm 0.01 \cdot 10^4$	$0.7 (\pm 0.2) \cdot 10^3$	0.040	$3 (\pm 1) \cdot 10^2$
Starting KCl/HCl ≈ 10					
11	2.7 ± 0.6	$1.45 \pm 0.02 \cdot 10^4$	$2.1 (\pm 0.2) \cdot 10^3$	0.029	$1.3 (\pm 0.1) \cdot 10^4$
12	7.30 ± 0.27	$2.16 \pm 0.03 \cdot 10^4$	$2.1 (\pm 0.2) \cdot 10^3$	0.046	$1.7 (\pm 0.2) \cdot 10^4$
13	22.1 ± 0.3	$2.12 \pm 0.03 \cdot 10^4$	$2.6 (\pm 0.3) \cdot 10^3$	0.044	$1.8 (\pm 0.2) \cdot 10^4$
14	3.68 ± 0.2	$2.10 \pm 0.03 \cdot 10^4$	$1.8 (\pm 0.1) \cdot 10^3$	0.045	$1.4 (\pm 0.1) \cdot 10^4$
15	21.8 ± 0.3	$2.34 \pm 0.04 \cdot 10^4$	$2.7 (\pm 0.7) \cdot 10^3$	0.049	$1.8 (\pm 0.5) \cdot 10^4$
16	3.16 ± 0.19	$1.95 \pm 0.03 \cdot 10^4$	$2.0 (\pm 0.2) \cdot 10^3$	0.041	$1.4 (\pm 0.2) \cdot 10^4$
17	4.55 ± 0.22	$2.03 \pm 0.03 \cdot 10^4$	$2.4 (\pm 0.3) \cdot 10^3$	0.042	$1.8 (\pm 0.4) \cdot 10^2$
Starting K/H = 5, 3.33					
18	33.9 ± 1.1	$1.69 \pm 0.02 \cdot 10^4$	$2.2 (\pm 0.3) \cdot 10^3$	0.035	$3.8 (\pm 0.2) \cdot 10^4$
19	99.5 ± 1.2	$1.89 \pm 0.02 \cdot 10^4$	$2.6 (\pm 0.3) \cdot 10^3$	0.039	$3.8 (\pm 0.5) \cdot 10^4$
20	5.0 ± 0.6	$1.54 \pm 0.02 \cdot 10^4$	$2.4 (\pm 0.2) \cdot 10^3$	0.031	$2.9 (\pm 0.3) \cdot 10^4$
21	5.79 ± 0.2	$1.99 \pm 0.03 \cdot 10^4$	$2.5 (\pm 0.5) \cdot 10^3$	0.041	$3.1 (\pm 0.4) \cdot 10^4$
22	87.5 ± 0.4	$2.11 \pm 0.03 \cdot 10^4$	$2.0 (\pm 0.2) \cdot 10^3$	0.045	$3.5 (\pm 0.3) \cdot 10^4$
23	25.6 ± 0.3	$1.94 \pm 0.03 \cdot 10^4$	$2.9 (\pm 0.3) \cdot 10^3$	0.039	$3.3 (\pm 0.7) \cdot 10^4$
24	10.2 ± 0.2	$2.13 \pm 0.03 \cdot 10^4$	$2.8 (\pm 1.1) \cdot 10^3$	0.044	$4 (\pm 2) \cdot 10^4$

Cl concentrations of the glass (quenched melt) portion of the phase mixture (Cl_g) were completed by using EPMA. The mass fraction of the brine relative to the phase mixture (mf_b) was calculated by relating the concentrations of chloride in the glass to chloride in the glass + brine phase mixture. C^b_{HCl} (ppm) is calculated from the mass transfer of alkalis between the melt and brine by using the starting compositions and masses of the melt and brine and the final composition of the melt. The experiments with the lowest concentration of HCl for each experimental condition were used to minimize the systematic uncertainty of the partitioning of Au in the phase mixture due to the strong relationship between HCl and Au solubility. Standard deviations of INAA measurements were calculated:

$$\%\ Uncertainty = 100 \cdot \sqrt{\frac{Peak\ Area \cdot 2 \cdot Background}{Peak\ Area}}.$$

Uncertainty in EPMA measurements are 1 sigma (σ) of the standard deviation of the mean, and uncertainty in HCL_b is calculated as a propagation of all uncertainties involved in the calculation (1 σ).

ppm, gold concentrations in the phase mixture < 4 ppm, and uncertainty in gold concentrations < 30% relative regress to yield a gold concentration of ≈1 ppm in a melt devoid of fluid inclusions (Fig. 4).

Individual glass fragments from select experiments (2, 17, and 24) were analyzed by using Secondary Ion Mass Spectrometry (SIMS) to supplement the gold analyses of the glass + brine phase mixture obtained by using INAA. SIMS analysis revealed variations in the concentration of gold in the glasses. The quenched glasses exhibited gold "nuggets," or volumes of increased gold concentration within the glass relative to the surrounding matrix glass. The Au concentrations in the nugget regions were ~1 order of magnitude greater than the glass matrix. Regions of elevated gold concentrations did not exhibit an equivalent increase in chloride, suggesting that the localized high gold concentrations are not derived from gold-bearing fluid inclusions. Rather, we suggest that the gold nuggets present within the quenched silicate glass are likely formed on quench, that is, the gold was homogeneously distributed throughout the melt and then exsolved from the melt during quench into the nugget regions. This interpretation is favored over an explanation involving localized precipitation of gold metal during the experiment because of the consistent results produced by bulk INAA analysis of the glass. This phenomenon has been observed for gold-bearing sulfide minerals (Jugo et al., 1999). Therefore, we think the best method of evaluating the solubility of gold in a silicate melt from SIMS data is to integrate the SIMS gold signal over time. Taking the average of all measurements suggests that the concentration of gold in the silicate melts at run conditions was ~0.9 ppm, broadly consistent with the results from INAA analyses of glass + brine phase mixtures.

The data suggest that the best estimate of gold concentration in the glass at run conditions is ~1 ppm. There is some reason to believe that there might be a weak dependence of the solubility of gold metal in the glass on the HCl concentration in

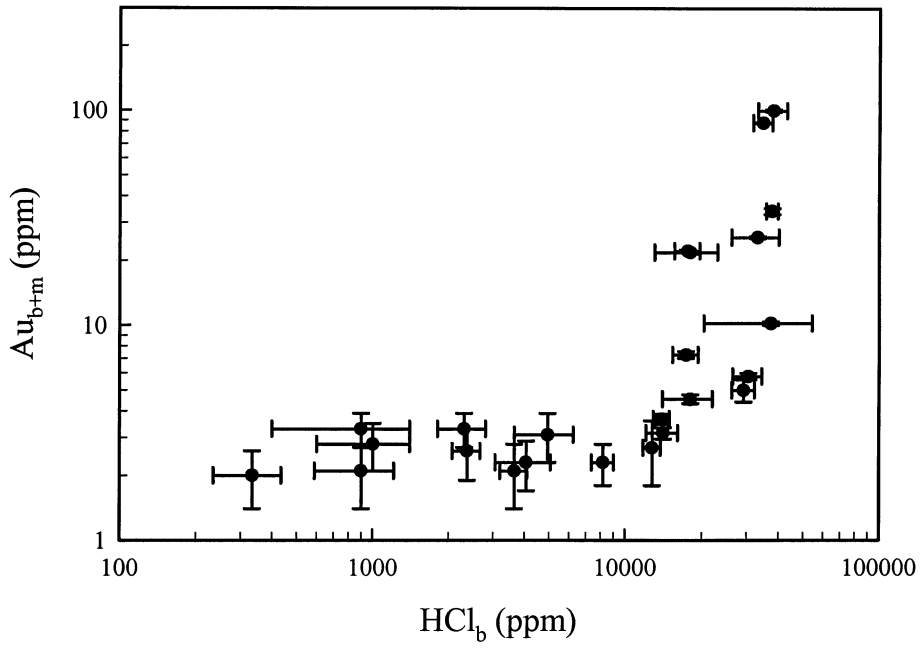

Fig. 3. INAA analyses for gold of the quenched glasses (phase mixtures, brine + melt) plotted against the calculated HCl concentration of the brine. The solubility of gold in the phase mixture is independent of HCl at low-HCl concentrations and varies directly with the HCl at high-HCl concentrations. The error bars are 1σ.

the brine, but at any reasonable HCl concentration, the gold solubility in the melt was on the order of 1 ppm. Further experiments, at other oxygen fugacities and higher concentrations of HCl in a coexisting MVP, are required to evaluate the potential importance of Au_2O, AuCl, and AuOH species in silicate melts.

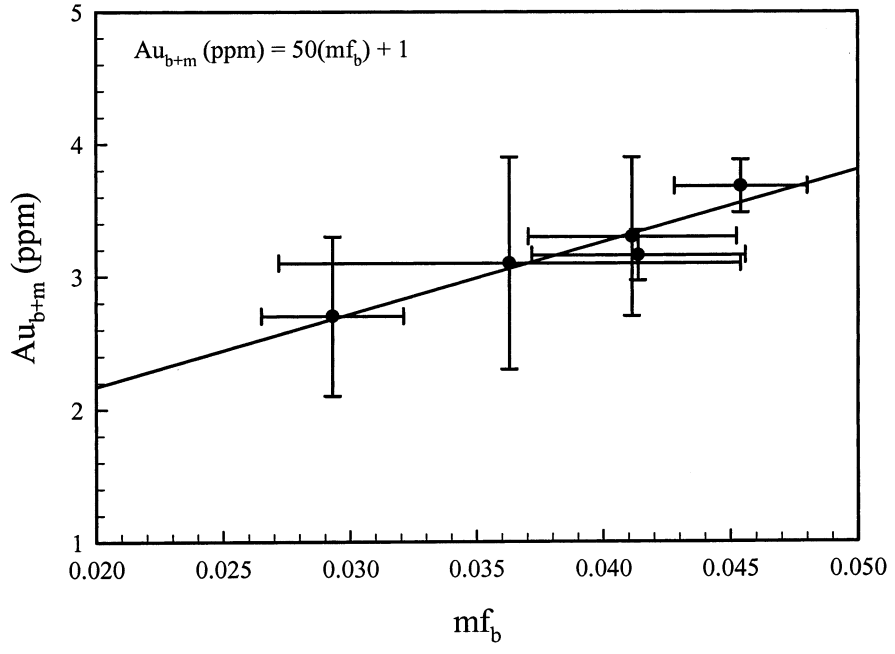

Fig. 4. Gold concentrations in the glass + brine phase mixtures plotted against the mass fraction of brine in the glasses (mf_b) for experiments with $> 4.2 \times 10^3$ and $< 1.4 \times 10^4$ ppm HCl in the brine. Extrapolating the results to mf_b = zero provided one means of determining the concentration of gold in a silicate melt at each experimental condition. Experiments with $> 1.4 \times 10^4$ ppm HCl were not used because of the strong relationship between [insert equation from page 46 here] and HCl. Linear regression (black solid line) of the data suggests that the solubility of gold in the silicate melts of these experiments is on the order of 1 ppm. The r^2 of the regression is 0.90.

Table 6. Calculated concentrations of gold in brine fluid inclusions contained in the glass + brine phase mixtures were obtained by using a gold concentration in the glass (log $C^g_{Au} = 0.0 \pm 0.2$ ppm; ppm is by weight).

Run	Log Au_b (ppm)	HCl_b (ppm)
1	1.5 (±0.3)	$3.7\ (\pm 0.4) \cdot 10^3$
2	1.8 (±0.4)	$5\ (\pm 1) \cdot 10^3$
3	1.6 (±0.3)	$2.4\ (\pm 0.3) \cdot 10^3$
4	1.7 (±0.3)	$2.3\ (\pm 0.5) \cdot 10^3$
5	1.8 (±0.4)	$0.9\ (\pm 0.5) \cdot 10^3$
6	1.5 (±0.3)	$4\ (\pm 1) \cdot 10^3$
7	1.5 (±0.3)	$8.2\ (\pm 0.8) \cdot 10^3$
8	1.4 (±0.3)	$0.9\ (\pm 0.3) \cdot 10^3$
9	1.6 (±0.3)	$1.0\ (\pm 0.4) \cdot 10^3$
10	1.4 (±0.3)	$3\ (\pm 1) \cdot 10^2$
11	1.8 (±0.4)	$1.3\ (\pm 0.1) \cdot 10^4$
12	2.1 (±0.4)	$1.7\ (\pm 0.2) \cdot 10^4$
13	2.7 (±0.5)	$1.8\ (\pm 0.2) \cdot 10^4$
14	1.8 (±0.4)	$1.4\ (\pm 0.1) \cdot 10^4$
15	2.6 (±0.5)	$1.8\ (\pm 0.5) \cdot 10^4$
16	1.7 (±0.3)	$1.4\ (\pm 0.2) \cdot 10^4$
17	1.9 (±0.4)	$1.8\ (\pm 0.4) \cdot 10^4$
18	3.0 (±0.6)	$3.8\ (\pm 0.2) \cdot 10^4$
19	3.4 (±0.7)	$3.8\ (\pm 0.5) \cdot 10^4$
20	2.1 (±0.4)	$2.9\ (\pm 0.3) \cdot 10^4$
21	2.1 (±0.4)	$3.1\ (\pm 0.4) \cdot 10^4$
22	3.3 (±0.7)	$3.5\ (\pm 0.3) \cdot 10^4$
23	2.8 (±0.6)	$3.3\ (\pm 0.7) \cdot 10^4$
24	2.3 (±0.5)	$4\ (\pm 2) \cdot 10^4$

Uncertainties presented for the concentrations of gold and HCl in brines are the standard deviations from the mean and are 1σ, respectively.

3.3.3. Gold solubility in a brine as a function of HCl concentration

The concentration of gold in a brine, C^b_{Au}, was calculated for each glass + brine phase mixture by using the best estimate of the solubility of gold metal determined for the glasses (≈1 ppm). The concentration of gold in the glass + brine phase mixture, C^{g+b}_{Au}, can be related through mass-balance constraints to C^b_{Au} by:

$$C^{g+b}_{Au} = (C^g_{Au} \cdot mf_g) + (C^b_{Au} \cdot mf_b) \quad (2)$$

where mf_b is the mass fraction of brine in the phase mixture, mf_g is the mass fraction of glass in the phase mixture and C^g_{Au} is the inferred concentration of gold in the glass. Rearranging Eqn. 2 to:

$$\left[\frac{C^{g+b}_{Au} - (C^g_{Au} \cdot mf_g)}{mf_b}\right] = C^b_{Au} \quad (3)$$

and calculating C^b_{Au} for the value of C^g_{Au} stated above, the solubility of gold in the brines of the experiments can be calculated (Table 6). The uncertainty associated with the calculated C^b_{Au} value from each run, on the order of 20% relative, is large because the uncertainty in C^g_{Au} is large.

The concentration of gold in the brine is presented as a function of C^b_{HCl} (Fig. 5). Two trends are apparent in the data, one at low C^b_{HCl}, 1.00×10^2 to 1.10×10^4 ppm, and one at higher values of C^b_{HCl}, $> 1.10 \times 10^4$ ppm. The solubility of gold in a brine at $C^b_{HCl} < 1.10 \times 10^4$ is $4(\pm 1) \times 10^1$ ppm (1σ standard deviation of the mean). The change in slope at ≈1.10×10^4 ppm HCl suggests a change in the speciation of gold in the brine. A line regressed through the data at low C^b_{HCl} displays a slope only slightly greater than zero, suggesting that gold solubility in a brine is not a function of $C^b_{HCl} < 1.10 \times 10^4$ ppm. Thus, gold-chloro complexes are most likely not the dominant species of gold in the brine at low C^b_{HCl}.

There is a correlation between HCl in the brine and gold solubility in the brine at $C^b_{HCl} > 1.10 \times 10^4$ ppm and can be represented by:

$$\log C^b_{Au} = 2.2 \cdot (\log C^b_{HCl}) - 7.2 \quad (4)$$

Regressing the data at high-HCl concentrations yields a slope of ~2, suggesting that the complex of gold in the brine under these conditions has a chloride-to-gold ratio of 2 : 1. At the experimental conditions of this study, the ability of the brine to ionize species is diminished, resulting in species that are associated and electrically neutral. Therefore, we suggest tentatively that $AuCl_2H$ (AuCl × HCl) is the dominant complex in the brine at high C^b_{HCl}.

The regression lines displayed in Figure 5 are based on the total concentration of gold in the brine and would, hence, be subjected to influence by all gold species present in the brine. For example, the slight increase in gold concentrations in the brine with increasing HCl for the low-HCl experiments, where a gold-chloro complex is not thought to be important, may be the result of the HCl-dependent $AuCl_2H$ species. At model HCl concentrations of 1000 and 5000 ppm, the concentrations of gold in the brine are calculated, respectively, as 35 and 44 ppm by using the equation for the regressed line. A non-chloro gold complex should not be affected by HCl concentrations in the brine, so the solubility of gold in the brine as a non-chloro species should be independent of HCl. Conversely, the slight increase in the gold solubility in the brine at $C^b_{HCl} < 1.1 \times 10^4$ ppm may be related to $AuCl_2H$. By using the linear regression for experiments at $C^b_{HCl} > 1.1 \times 10^4$ ppm, Eqn. 4, the proportion of gold added to the non-chloro gold would be 0.3 and 9 ppm at model C^b_{HCl} of 1000 and 5000 ppm, respectively. Therefore, the slight increase in gold solubility for $C^b_{HCl} < 1.1 \times 10^4$ ppm is consistent with the addition of gold as $AuCl_2H$ to the non-chloro gold.

3.4. Thermodynamic Modeling

3.4.1. Partition coefficients for gold between a sulfur-free brine and melt

Partition coefficients for gold between brine and melt, $D^{b/m}_{Au}$, have been determined at 800°C, 100 MPa, log $f_{O_2} = -14$, KCl/NaCl = 0.500–1.00, and KCl/HCl = 3.20–100. Representation of the partition coefficients in this study is problematic because the preliminary analysis suggests that the solubility of gold in the brine is nearly independent of HCl for $C^b_{HCl} < 1.10 \times 10^4$ ppm in the brine, but dependent on HCl at $C^b_{HCl} > 1.10 \times 10^4$ ppm. $D^{b/m}_{Au}$ for low-HCl, sulfur-free brines is constant = $4(\pm 1) \times 10^1$ from 3×10^3 to 1.1×10^4 ppm HCl. It is evident that gold exhibits a preference for the brine relative to melt over the range of conditions examined in this study. $D^{b/m}_{Au}$ varies with C^b_{HCl} according to:

$$\log (D^{b/m}_{Au}) = 2.2 \cdot \log(C^b_{HCl}) - 7.2 \quad (5)$$

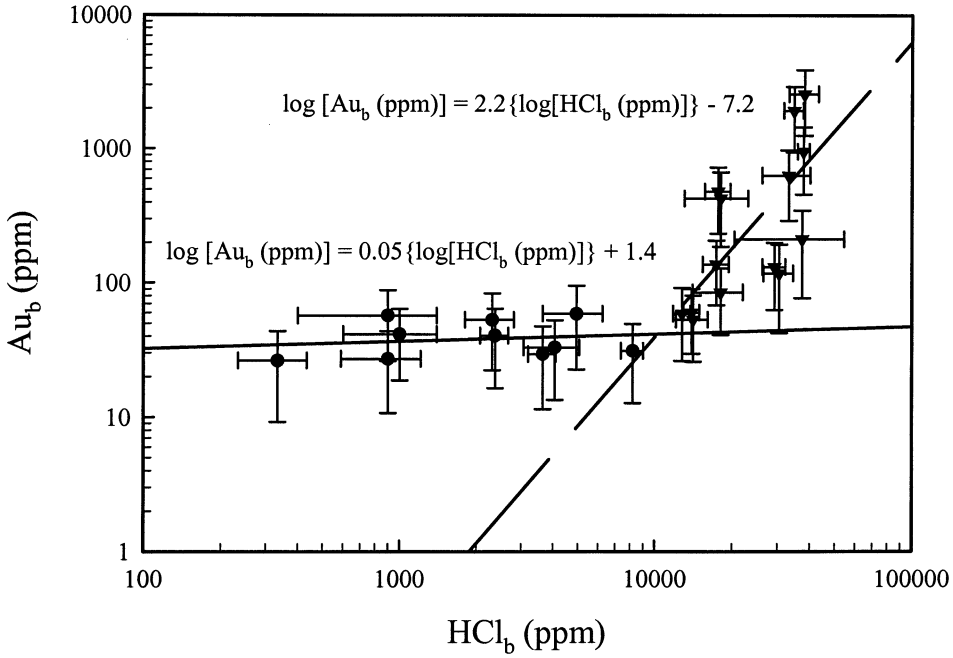

Fig. 5. Solubility of gold in a brine as a function of HCl. Two trends are apparent: First, gold solubility in a brine with $< 1.10 \times 10^4$ ppm HCl is independent of the HCl concentration in the brine, and thus the existence of a dominant gold-chloro complex is unlikely (solid line). Second, at HCl concentrations in the brine $> 1.10 \times 10^4$ ppm, gold solubility is affected strongly by HCl (dashed line). The slope of ~2 in this region indicates a Cl to Au ratio of ~2 in the dominant Au-bearing complex, leading us to conclude that the $AuCl_2H$ complex is dominant in a brine at HCl $> 1.10 \times 10^4$ ppm. Uncertainties are 1σ and calculated based on the propagation of error for each measurement used to calculate gold and HCl, respectively.

for brine HCl concentration $> 1.10 \times 10^4$ ppm. These partition coefficients indicate that gold will partition strongly into a coexisting brine relative to a silicate melt over the entire range of C^b_{HCl} studied, even in the absence of sulfur, but the partitioning increases strongly for $C^b_{HCl} > 1.1 \times 10^4$ ppm. Therefore, the concentration of HCl in the brine cannot only be a determining factor in the extent to which gold will partition into a brine from a melt, but ultimately, it is an important factor in the efficiency with which gold is transported by the brine.

3.4.2. Equilibrium constants

The solubility of gold in a brine with HCl $< 1.10 \times 10^4$ ppm was not affected by C^b_{HCl}, so it was concluded that a gold-chloride complex was not the dominant species present (although a small proportion of the total gold in the brine may be chloride-complexed). This study was conducted in a sulfur-free system, so that any Au-sulfur species can be discounted. It appears that a non-sulfur, non-chloride species is dominant in a low-HCl sulfur-free brine. Unfortunately, the dominant gold species in the brine at low-HCl conditions was not identified. However, the strong relationship between the concentrations of gold and HCl in the brine (Fig. 5) illustrates the important role of solution acidity in controlling gold solubility. A brine with $C^b_{HCl} > 1.1 \times 10^4$ ppm can accommodate a significant concentration of gold, with most being complexed as $AuCl_2H$ (AuCl × HCl), and thus the brine is a reasonable candidate for the transport of gold from a crystallizing silicate melt into an overlying hydrothermal system. To explain the transfer of gold between a silicate melt and sulfur-free brine, the following equilibrium (Eqn. 6), based on the slope of ~2 between log (C^b_{Au}) and log (C^b_{HCl}) of the brine, is proposed:

$$AuO_{0.5\,(m)} + 2\ HCl_{(b)} = AuCl_2H_{(b)} + 1/2\ H_2O_{(sys)} \qquad (6)$$

The solubility of gold in a high-temperature aqueous phase may be a function of $f^{sys}_{O_2}$, C^b_{Cl} and C^b_{HCl}. In this study, water activity and oxygen fugacity were constant, but the data are also consistent with the equilibrium:

$$\frac{1}{4}\,O_2 + Au_{(metal)} + 2\ HCl_{(b)} = AuCl_2H_{(b)} + \frac{1}{2}\,H_2O \qquad (7)$$

The dependence of the equilibria (Eqn. 6, 7) on HCl can be illustrated by noting that $AuCl_2H$ is essentially AuCl × HCl. Coupling this with the known changes in the dielectric constant of the brine at high temperature, an associated and electrically neutral species becomes the most likely gold-chloro species. Thus the supposition that the dominant gold-chloro complex in the brine, at $C^b_{HCl} > 1.10 \times 10^4$ ppm, was $AuCl_2H$ is supported by the equilibria in addition to the intuitive reasoning with regard to the dielectric constant of the fluid.

An equilibrium constant, K (T,P), for Eqn. 6 can be expressed as:

$$K_{Eq.6}\,(800°C,\ 100\ MPa) = \left(\frac{a^b_{AuCl_2H} \cdot (f^{sys}_{H_2O})^{0.5}}{(a^b_{HCl})^2 \cdot a^m_{AuO_{0.5}}}\right) \qquad (8)$$

where $a^b_{AuCl_2H}$, $a^m_{AuO_{0.5}}$ and a^b_{HCl} are the activities of the $AuCl_2H$ component in the brine, $AuO_{0.5}$ component in the melt, and HCl in the brine, respectively. $f^{sys}_{H_2O}$ is set by the

Table 7. Apparent equilibrium constants K′ (T,P) for equilibria (6) and (7) presented for the moderate (KCl/HCl = 10) and high (KCl/HCl = 5 and 3) starting HCl concentrations in the brine.

	Starting KCl/HCl = 10	Starting KCl/HCl = 5, 3	All Experiments
Log $K'_{Eq.6}$	$2.0\ (\pm 0.8) \cdot 10^{-5}$	$2.2\ (\pm 0.9) \cdot 10^{-5}$	$2.1\ (\pm 0.9) \cdot 10^{-5}$
Log $K'_{Eq.7}$	0.07 ± 0.03	0.07 ± 0.03	0.07 ± 0.03

$f^{sys}_{O_2}$, $f^{sys}_{H_2O}$ and α^{metal}_{Au} are controlled by the conditions of the experiment and are $1.04 \cdot 10^{-14}$, 570, and 1.0, respectively. C^b_{HCl}, C^m_{Au} and $C^b_{AuCl_2H}$ were obtained following the methods outlined in the text and are in ppm (by weight).

conditions of the experiments at 570 bars. However, the activities of the other components cannot be specified because the activity coefficients (γ^x_i) are unknown; thus the activity coefficients are incorporated into an apparent equilibrium constant, K′ (T,P), which can be expressed as:

$$K'_{Eq.6}(800°C,\ 100\ MPa) = \left(\frac{C^b_{AuCl_2H} \cdot (f^{sys}_{H_2O})^{0.5}}{(C^b_{HCl})^2 \cdot C^m_{AuO_{0.5}}} \right) \qquad (9)$$

where $C^b_{AuCl_2H}$, $C^m_{AuO_{0.5}}$, and C^b_{HCl} are the concentrations of the $AuCl_2H$ component in the brine, $AuO_{0.5}$ component in the melt, and HCl in the brine, respectively. Eqn. 9 is applicable over the range of C^b_{HCl} from 1.1×10^4 to 4.0×10^4 ppm and was calculated for the two starting brine KCl/HCl values that produced brine with $> 1.1 \times 10^4$ ppm HCl. Moderate-HCl (1.28×10^4 to 1.81×10^4 ppm), and high-HCl (2.92×10^4 to 3.82×10^4 ppm) experiments produced $K'_{Eq.6}$ of $2.0(\pm 0.8) \times 10^{-5}$ and $2.2(\pm 0.9) \times 10^{-5}$ (uncertainties are 1σ), respectively, and considering all experiments with HCl $> 1.1 \times 10^4$ ppm, a $K'_{Eq.6} = 2.1(\pm 0.9) \times 10^{-5}$ was calculated (Table 7).

An equilibrium constant for Eqn. 7 can be written as

$$K_{Eq.7}(800°C,\ 100\ MPa) = \left(\frac{a^b_{AuCl_2H} + (f^{sys}_{H_2O})^{0.5}}{a^{metal}_{Au} \cdot (f^{sys}_{O_2})^{0.25} \cdot (a^b_{HCl})^2} \right) \qquad (10)$$

where a^{metal}_{Au} and $f^{sys}_{O_2}$ are the activities of gold in the gold metal capsule and fugacity of O_2 in the system. The apparent equilibrium constant for Eqn. 7 is written as:

$$K_{Eq.7}(800°C,\ 100\ MPa) = \left(\frac{C^b_{AuCl_2H} + (f^{sys}_{H_2O})^{0.5}}{a^{metal}_{Au} \cdot (f^{sys}_{O_2})^{0.25} \cdot (C^b_{HCl})^2} \right) \qquad (11)$$

Eqn. 11 is applicable only for the range of C^b_{HCl} of 1.1×10^4 to 4.0×10^4 ppm. Values of $K'_{Eq.7}$ for moderate-HCl and high-HCl experiments were calculated as 0.07 ± 0.03 and 0.07 ± 0.03, respectively; whereas $K'_{Eq.7} = 0.07 \pm 0.03$ for all experiments with $C^b_{HCl} > 1.1 \times 10^4$ ppm (Table 7). Neither $K'_{Eq.6}$ nor $K'_{Eq.7}$ was calculated for the low-HCl experiments, because the prevalent gold species in the brine was not determined.

4. DISCUSSION

4.1. Solubility of Gold in Natural Silicate Melts

Potential sources for gold in many ore deposits include, but are not limited to, a crystallizing magma, country rocks, flux from a deep-seated "exotic" fluid, or a combination of sources. Knowledge of the solubility of gold in a silicate melt is of great importance in evaluating the potential for a crystallizing magma to be a source of ore metal for a gold-bearing ore deposit.

The solubility of gold in a silicate melt in equilibrium with a high-salinity brine was determined to be ≈1 ppm. The relationship between the concentration of gold in the quenched glass and HCl in the brine, for $C^b_{HCl} > 1.10 \times 10^4$, was problematic because even a slight difference in HCl would alter systematically the inferred gold solubility in the melt. Low-HCl experiments were not affected greatly, because the concentrations of HCl in the brine were only a few thousand ppm. Moderate- and high-HCl experiments produced brines, which ranged from 1×10^4 to 4×10^4 ppm HCl, so extraction of gold concentrations in the melt was not possible. Accordingly, experiments with the lowest HCl concentrations for the moderate- and high-HCl experiments were chosen to minimize the effect of gold concentrations in the brines. Comparing the extrapolated gold solubility in a silicate-melt, sulfur-free assemblage with the measured solubility of gold in quenched glasses (by using SIMS), the data overlap when uncertainties are considered and further suggest that gold solubility in a silicate melt was ≈1 ppm.

A preliminary study by Candela et al. (1996) determined the solubility of gold in a haplogranitic melt in the gold metal + vapor + silicate melt assemblage to be 2 to 4 ppm at 800°C, 140 MPa, log $f^{sys}_{O_2} = -13.3$ and KCl/HCl = 50. Jugo et al. (1999) reported a solubility of 4.1 ± 2.4 (1σ) ppm gold in a haplogranitic melt ($Qtz_{0.26}Ab_{0.32}Or_{0.34}An_{0.08}$) in a melt + pyrrhotite + intermediate solid solution + gold metal assemblage at 850°C, 100 MPa, log $f^{sys}_{O_2} = -13.2$ and KCl/HCl = 7.5. It must be noted that the experiments of Candela et al. (1996) and Jugo et al. (1999) contained vapors and not brines; hence the systems had much lower chloride contents relative to the work presented here. Hoosain and Baker (1996) determined the solubility of gold in a metaluminous rhyolite and a water-saturated metaluminous rhyolite with 1.2 wt.% fluorine at 800°C, 150 MPa. They found the concentration of gold was below detection (< 0.1 ppm) in the metaluminous rhyolite and 0.298 ± 0.25 ppm in the rhyolite with 1.2 wt.% fluorine. Our data indicating ≈1 ppm gold in the melt falls within the range of concentrations presented above (≈0.3–4 ppm) and thus compare favorably with these investigators. Apparently small changes in temperature, pressure, total chloride, total sulfur, and melt composition have only a small effect on the solubility of gold in granitic melts.

We propose that the gold present in silicate melts, at the conditions of the experiments, is dominated by the $AuO_{0.5}$ species. Further, variations in water activity, chloride concentration, or perhaps more importantly, oxygen fugacity may affect gold speciation in the melt. For example, melts with greater proportions of H_2O relative to HCl may allow for a larger proportion of gold being complexed as AuCl species in the melt by the equilibrium:

$$AuO^m_{0.5} + HCl^b = AuCl^m + 1/2\ H_2O^m \qquad (12)$$

For a review of the speciation of water in silicate melts see Stolper (1982), Kohn et al. (1989), Ihinger et al. (1994), and

McMillan (1994). The possibility that some gold in a silicate melt is present as Au^o should also be considered. Ultimately, additional experimental studies over a range of conditions are required to address these questions.

In a study of gold abundance in natural systems, Connors et al. (1993) analyzed 129 glassy silicic volcanic rocks for gold and found the majority of them ($n = 113$) contained ≤ 1 ppb gold (by weight). They inferred that granitic systems associated with gold deposits may be elevated in initial gold content but probably not > 4 ppb. Thus gold contents of magmas need not be elevated drastically to produce a magmatic-hydrothermal gold deposit. Our results indicate gold solubility in a silicate melt of $\approx$1 ppm at gold metal saturation. By using a gold metal activity scale (i.e., the activity of gold in metal in equilibrium with the melt), together with the concentration of gold in a melt in equilibrium with gold metal, the activity of gold in the volcanic rocks (from Connors et al., 1993) can be inferred by comparing the concentration of gold in those rocks to the aforementioned standard state. Based on this methodology, the activity of gold in those magmas is on the order of 10^{-3}. Thus on this defined activity scale, the activity of gold in the volcanic rocks analyzed by Connors et al. (1993) is approximately three orders of magnitude below that required for gold metal saturation. This provides a fair estimate of the activity of gold in these systems, which is useful in applying experimental data to natural systems.

4.2. Solubility and Speciation of Gold in a High-Salinity, Sulfur-Free Brine

Many studies have evaluated the solubility and speciation of gold in the low- to moderate-temperature, subsolidus hydrothermal environment. It has been proposed that bisulfide, hydroxide, chloride, and other species transport gold under these conditions (Benning and Seward, 1996; Gammons and Williams-Jones, 1997; Gibert et al., 1998). The role of sulfur is significant in controlling gold concentration and speciation in mesothermal and epithermal environments. Specifically, reduced systems may transport gold as $Au(HS)_2^-$ and AuHS at high and low pH, respectively (Renders and Seward, 1989; Zotov et al.,1994; Benning and Seward, 1996; Gammons and Williams-Jones, 1997; Gibert et al., 1998). However, gold-chloride complexes, specifically $Au(Cl)_2^-$, probably become dominant as solution acidity and temperature are increased (Gammons and Williams-Jones, 1997). Pan and Wood (1991) demonstrated that the $Au(Cl)_2^-$ complex was present above 100°C and under acidic conditions (2–5 *m* HCl) by using Raman Spectroscopic methods.

The results in the sulfur-free, brine + melt + metallic gold assemblage indicate that a significant proportion of gold is not chloride-complexed in brines with $< 1.10 \times 10^4$ ppm HCl and that gold concentrations increase directly with C^b_{HCl} and are dominated by the $AuCl_2H$ complex at $C^b_{HCl} > 1.10 \times 10^4$ ppm. A study conducted by Zotov et al. (1994) at 450°C and 40 to 100 MPa observed a similar trend. They found gold solubility was independent of HCl in the HCl-H_2O system at low total chloride (0.0006–0.06 *m*) and that solubility was governed by the AuOH complex. The addition of chloride to the system, as KCl (3.31 *m*) or NaCl (1.02 *m*), caused the gold solubility to change directly with increasing HCl and increasing chloride. Zotov et al. (1994) state that in a sulfur-free system, AuOH and $Au(Cl)_2^-$ are the complexes prevalent at low- and high-HCl conditions, respectively. Trends in the data from this study (Fig. 5; Zotov et al., 1994, Fig. 5.3 therein) are consistent, so it is reasonable to assume a portion of the gold present in the low-HCl brines in this study was complexed as AuOH.

Few experimental data are available on gold speciation and solubility under magmatic conditions. Loucks and Mavrogenes (1999) found high concentrations of gold in a sulfidic aqueous fluid in eight experiments performed over a large range of temperatures (550–725°C) and pressure (110–400 MPa). Although they refer to their aqueous solution as a brine, chloride concentrations were on the order of 0 to 1 *m* total chloride, significantly below the chloride concentrations of the brines in this study. They reported results from only one experiment at 725°C and 110 MPa, conditions close to those of this study, and found a gold solubility of 135 $\pm$ 13 ppm, but they did not report an equilibrium HCl concentration for the experiment. Thus it is difficult to evaluate their results relative to ours. However, we chose to compare the low-HCl experiments (1000–5000 ppm) of this study to Loucks and Mavrogenes (1999) because the starting HCl concentrations of their solutions were $\approx$5000 ppm. The results from this study, at 800°C and 100 MPa, indicate the concentration of gold in the low-HCl realm of a high-salinity, sulfur-free brine is lower than that found by Loucks and Mavrogenes (1999) in a lower-salinity, sulfur-rich aqueous fluid. The elevated concentrations may be a result of gold-sulfo complexes; however, the lack of experimental control in the Loucks and Mavrogenes (1999) study, coupled with the fact that data are only presented for one experiment, require caution when interpreting their results. Rather we prefer to consider our data to be broadly consistent with the Loucks and Mavrogenes (1999) result.

Based on the experimental work of Zotov et al. (1994) and the theoretical model of Tossell (1996), their results are not inconsistent with a large portion of gold in the aqueous phases being complexed as AuOH in sulfur-free, low-HCl brines. If a portion of the gold occurs as AuOH, then the equilibrium:

$$AuOH^b + 2\ HCl^b = AuCl_2H^b + H_2O^b \qquad (13)$$

may explain the transition to the $AuCl_2H$ species present in the brine at moderate to high C^b_{HCl} conditions.

4.3. Generation of an Acidic Brine Capable of Transporting $AuCl_2H$

The solubility and speciation of gold in a brine is controlled strongly by the concentration of HCl in the brine. The solubility of gold in a brine at gold metal saturation is $\approx$40 ppm at HCl concentrations $< 1.1 \times 10^4$ ppm and ranges from 40 to $\approx$900 ppm at HCl concentrations of 1.1×10^4 to 4.0×10^4 ppm HCl, respectively. We have determined the speciation of the dominant gold complex in the 1.1×10^4 to 4.0×10^4 ppm HCl range to be $AuCl_2H$. However, is it geologically reasonable to have a brine with $> 1.1 \times 10^4$ ppm HCl coexisting with a silicate melt?

Williams et al. (1997) performed experiments in the high-silica rhyolite melt-vapor-brine system to investigate the exchange of hydrogen, potassium, and sodium between melts and volatile phases at 800°C and 100 MPa. KCl/HCl and, ulti-

mately, the C^b_{HCl} of the brine can be calculated based on the composition of the coexisting silicate melt by using the equilibrium constant for the brine-melt equilibrium (their Table 4) and the equation:

$$\log\left[\frac{KCl}{HCl}\right] = \log\left[\frac{C^m_K}{K^{b/m}_{H,K} \cdot \Sigma Alk^m \cdot (ASI - 1)}\right] \quad (14)$$

(their Eqn. A6), where $K^{b/m}_{H,K}$ and ΣAlk^m are the equilibrium constant for the hydrogen-potassium exchange and the summation of total alkalis (K, Na, and Ca) in the melt, respectively. This model suggests that a silicate melt with an ASI = 1.01 and $C^m_K/\Sigma Alk^m = 0.5$ will exsolve a brine with a KCl/HCl = 15; at 70 wt.% NaCl (eq.) this yields $\approx 1.1 \times 10^4$ ppm HCl. Keeping $C^m_K/\Sigma Alk^m$ constant and increasing the ASI of the silicate melt to 1.04 will decrease the KCl/HCl to 4.6 and increase the C^b_{HCl} to $\approx 3.7 \times 10^4$ ppm. See Williams et al. (1997) for a thorough discussion of the model. Cooling, homogeneous magmatic volatile phases with KCl/HCl of 15 and 4.6 will pass from potassium feldspar stable to muscovite (+ quartz) stable at ≈425 and ≈470°C, respectively (Frank et al., 1998). This is consistent with the alteration assemblages and the temperatures inferred for brine-dominated alteration envelopes in fossil magmatic-hydrothermal systems. Therefore, the concentrations of HCl in magmatic brines required for high gold concentrations (as $AuCl_2H$) are not unreasonable, according to the data of Williams et al. (1997) and Frank et al. (1998).

5. IMPLICATIONS

5.1. Application to Natural Systems

Silicate melts may become saturated with respect to a MVP on emplacement in the upper levels of the crust (due to a decrease in load pressure) and/or during crystallization of a dominantly anhydrous supersolidus phase assemblage. The MVP may be a brine, vapor, brine + vapor phase mixture, or supercritical fluid and will exsolve from the melt once saturation occurs. The MVP can transport solutes and heat to the surrounding associated hydrothermal system. The association of brines with silicate melts has been well demonstrated in a number of cases, such as Questa, New Mexico (Cline and Bodnar, 1994), the Capitan pluton, New Mexico (Ratajeski and Campbell, 1994; Dunbar et al., 1996), and the Mariktikan pluton, western Transbaikalia (Reyf, 1997). Conversely, the genesis of a brine capable of transporting ore metals is not restricted to a brine exsolving directly from a crystallizing melt. The large immiscibility region in the NaCl-KCl-H_2O system dictates that a vapor + brine pair will be present over a large range of bulk salinities (≈5–68 wt.% NaCl (eq.) at 800°C; Chou et al., 1992; Sterner et al., 1992; Anderko and Pitzer, 1993). Therefore, any NaCl-KCl-H_2O or similar aqueous phase(s) exsolving from a melt at 800°C and 100 MPa with ≈5 to 68 wt.% NaCl (eq.) will yield a two-phase mixture of vapor + brine. Another way to produce a vapor + brine pair in magmatic-hydrothermal systems is by the unmixing of a supercritical fluid due to a decrease in pressure.

In previous sections of this paper it was demonstrated that a large concentration of gold can be scavenged from a crystallizing melt, concentrated, and transported to an area of deposition by a brine. One of the largest hydrothermal gold mines is the porphyry-gold system at Grasberg, Irian Jaya, Indonesia. At Grasberg, Harrison (1999) has detailed the close association between igneous rocks and high-temperature (> 600°C) brine fluid inclusions and gold mineralization. Harrison concluded that a high-temperature, highly-saline fluid, > 60 wt.% NaCl (eq.), exsolved from the intrusion and precipitated the proximal ore. Ulrich et al. (1999) conducted a Laser Ablation ICP-MS study on individual fluid inclusions from Grasberg and Bajo de la Alumbrera. They found that brine inclusions from Grasberg and Bajo de la Alumbrera had salinities of 68 to 76 and 58 to 65 wt.% NaCl (eq.) and homogenization temperatures of > 600 and 550 to 650°C, respectively. The Au/Cu concentrations in high-temperature brine inclusions from these deposits were identical to the Au/Cu values of the bulk ore; thus they concluded that the bulk metal budgets of such deposits were controlled primarily by the composition of the incoming high-temperature brines. These studies provide strong evidence for the importance of gold-brine-melt equilibria and their applicability to natural systems.

A reaction that may be important in gold deposition at high temperature from high HCl brines is:

$$AuCl_2H_{brine} + 1/2\ H_2O \rightarrow Au^0 + 2\ HCl + 1/4\ O_2 \quad (15)$$

Examination of Eqn. 15 illustrates the importance of acidity and dilution as possible precipitation mechanisms for gold. Application of Le Châtelier's principle indicates that a decrease in the HCl concentration of the brine will induce precipitation of gold. Wall rock-brine alteration can act as a proton sink and neutralize the brine (Frank et al., 1998), causing gold metal to precipitate. A 70 wt.% NaCl (eq.) brine with ≈3.8 wt.% HCl will contain ≈750 ppm gold at gold metal saturation. A threefold drop in the concentration of HCl (to ≈1.2 wt.%) will drop the concentration of gold in the brine to ≈60 ppm. Therefore, ~90% of gold in a brine may be precipitated over this range of HCl concentrations. Coupling wall rock alteration with dilution of the brine by a flux of meteoric water into the hydrothermal system could cause significant gold precipitation and contribute to a high-grade porphyry gold deposit. Although either a decrease in the acidity or chloride concentration of a brine may be an efficient mechanism for ore precipitation, the two operating together may be responsible for giant gold deposits.

6. CONCLUSIONS

Experiments conducted at 800°C, 100 MPa and log $f_{O_2} = -14.0$ have demonstrated that gold solubility, speciation, and partitioning in a sulfur-free, brine-silicate melt-metallic gold system are controlled strongly by the HCl concentration of the brine. The solubility of gold in a silicate melt was found to be ≈1 ppm at gold metal saturation at HCl concentrations in the brine between 3×10^3 and 4.0×10^4 ppm. The solubility of gold in a brine, 70 wt.% NaCl (eq.), was ≈40 ppm and was independent of HCl for HCl concentrations in the brine of 3×10^3 to 1.1×10^4 ppm. We were not able to determine the speciation of gold at low-HCl conditions ($< 1.1 \times 10^4$ ppm) but were able to eliminate gold-chloro complexes as a possibility. For HCl brine concentrations ranging from 1.1×10^4 to 4.0×10^4 ppm, the solubility of gold in a brine increased from 40 to 840 ppm. The relationship between HCl and gold is consistent with $AuCl_2H$ being the dominant species of gold in

brines with $> 1.1 \times 10^4$ ppm HCl. Calculated partition coefficients, $D_{Au}^{b/m}$, for gold between a brine and melt changed from 40 to 840 at HCl concentrations in the brine of 3×10^3 and 4.0×10^4 ppm, respectively. The variation seen in the $D_{Au}^{b/m}$ as a function of HCl illustrates the need for thermodynamically accurate equilibrium constants. Apparent equilibrium constants, K′ (T, P), were determined for the pertinent equilibria in this study and allow for the accurate modeling of gold in magmatic-hydrothermal ore environments. The results of this study indicate that a substantial quantity of gold can be scavenged from a silicate melt by a high-HCl brine, although a low-HCl brine is capable of transporting a considerable amount of gold into an associated magmatic-hydrothermal system as well. Our results also imply that a significant amount of gold can be transported by a brine in the magmatic-hydrothermal environment regardless of the fugacities of sulfur-bearing species.

Acknowledgments— Support for this project was provided by the National Science Foundation [EAR 9506631 (PAC and PMP); EAR 9805313 (PAC and PMP); EAR 9810244 (PAC, PMP, and others)], Sigma Xi Grants in Aid of Research (MRF), BHP Student Research Grant from the Society of Economic Geologists (MRF), and the Department of Energy Research Reactor sharing program [DE-FG02-95NE38135]. We thank Rick Hervig (Arizona State University) for SIMS analyses and thoughtful discussions of the benefits and pitfalls of those analyses, Tom Williams for assistance in the early stages of this project, and Gary Cygan for many helpful discussions regarding hydrothermal geochemistry. GCA reviews by Scott Wood, A.E. Williams-Jones, and an anonymous reviewer improved this manuscript considerably and are greatly appreciated. MRF would like to dedicate this paper to Robert Frank who passed away during its completion.

Associate editor: S. Wood

REFERENCES

Anderko A. and Pitzer K. S. (1993) Equation-of-state representation of phase equilibria and volumetric properties of the system NaCl-H_2O above 573 K. *Geochim. Cosmochim. Acta* **57,** 1657–1680.

Benning L. G. and Seward T. M. (1996) Hydrosulfide complexing of gold(I) in hydrothermal solutions from 150 to 500°C and 500 to 1500 bars. *Geochim. Cosmochim. Acta* **60,** 1849–1872.

Bodnar R. J., Burnham C. W., and Sterner S. M. (1985) Synthetic fluid inclusions in natural quartz. III. Determination of phase equilibrium properties in the system H_2O-NaCl to 1000°C and 1500 bars. *Geochim. Cosmochim. Acta* **49,** 1861–1873.

Burnham C. W. (1979) Magmas and hydrothermal fluids. In *Geochemistry of Hydrothermal Ore Deposits* (ed. H. L. Barnes), pp. 71–136, New York, Wiley.

Candela P. A. (1990) Theoretical constraints on the chemistry of the magmatic aqueous phase. *Geol. Soc. Am. Spec. Paper* **246,** 11–20.

Candela P. A. and Holland H. D. (1984) The partitioning of copper and molybdenum between silicate melts and aqueous fluids. *Geochim. Cosmochim. Acta* **48,** 373–380.

Candela P. A. and Piccoli P. M. (1995) Model ore-metal partitioning from melts into vapor and vapor/melt mixtures. In *Magmas, Fluids, and Ore Deposits* (ed. J. F. H. Thompson), *Mineral. Assoc. Can.* **23,** 101–127.

Candela P. A., Piccoli P. M., and Williams T. J. (1996) Preliminary study of gold metal partitioning in a sulfur-free, high oxygen fugacity melt/volatile phase system. *GSA Ann. Meeting Abstracts with Programs.* **28,** 402.

Chou I. (1987) Oxygen buffer hydrogen sensor techniques at elevated pressures and temperatures. In *Hydrothermal Experimental Techniques* (eds. G. C. Ulmer and H. L. Barnes), pp. 61–99. Wiley, NY.

Chou I., Sterner S. M., and Pitzer K. S. (1992) Phase relations in the system NaCl-KCl-H_2O: IV. Differential thermal analysis of the sylvite liquidus in the KCl-H_2O binary, the liquidus in the NaCl-KCl-H_2O ternary, and the solidus in the NaCl-KCl binary to 2 kb pressure, and a summary of experimental data for thermodynamic-*PTX* analysis of solid-liquid equilibria at elevated. P-T Conditions. *Geochim. Cosmochim. Acta* **56,** 2281–2293.

Cline J. S. and Bodnar R. J. (1994) Direct evolution of brine from a crystallizing silicic melt at the Questa, New Mexico, molybdenum deposit. *Econ. Geol.* **89,** 1780–1802.

Connors K. A., Noble D. C., Bussey S. D., and Weiss S. I. (1993) Initial gold contents of silicic volcanic rocks: Bearing on the behavior of gold in magmatic systems. *Geology* **21,** 937–940.

Dunbar N. L., Campbell A. R., and Candela P. A. (1996) Physical, chemical, and mineralogical evidence for magmatic fluid migration within the Capitan Pluton, southeastern New Mexico. *Geol. Soc. Am. Bull.* **3,** 318–333.

Frank M. R., Candela P. A., and Piccoli P. M. (1998) K-feldspar-muscovite-andalusite-quartz-brine phase equilibria: An experimental study at 25 to 60 MPa and 400 to 550°C. *Geochim. Cosmochim. Acta* **62,** 3717–3727.

Gammons C. H. and Williams-Jones A. E. (1997) Chemical mobility of gold in the Porphyry-Epithermal environment. *Econ. Geol.* **92,** 45–59.

Gibert F., Pascal M-L., and Pichavant M. (1998) Gold solubility and speciation in hydrothermal solutions: Experimental study of the stability of hydrosulphide complex of gold ($AuHS^o$) at 350 to 450°C and 500 bars. *Geochim. Cosmochim. Acta* **62,** 2931–2947.

Glascock M. D. (1998) Activation analysis. In *Instrumental Multi-Element Chemical Analysis* (ed. Z. B. Alfassi), pp. 93–150, Kluwer Academic Publishers, Dordrecht, The Netherlands.

Harrison J. S. (1999) Hydrothermal alteration and fluid evolution of the Grasberg porphyry Cu-Au deposit, Irian Jaya, Indonesia. Unpubl. M.S. thesis. University of Texas at Austin.

Hedenquist J. W., Arribas A. Jr., and Reynolds T. J. (1998) Evolution of an intrusion-centered hydrothermal system: Far Southeast-Lepanto porphyry and epithermal Cu-Au deposits, Philippines. *Econ. Geol.* **93,** 373–404.

Heinrich C. A., Ryan C. G., Mernagh T. P., and Eadington P. J. (1992) Segregation of ore metals between magmatic brine and vapor. *Econ. Geol.* **87,** 1566–1583.

Holland H. D. (1972) Granites, solutions, and base metal deposits. *Econ. Geol.* **67,** 281–301.

Hoosain L. and Baker D. R. (1996) Solubility of gold in two granitic melts and its partitioning between sulfides and melt. *GAC-MAC Program with Abstracts* **21,** A-45.

Ihinger P. D., Hervig R. L., and McMillian P. F. (1994) Analytical methods for volatiles in glasses. In: Volatiles in Magmas (ed. M. R. Carroll and J. R. Holloway), *Mineral. Soc. Am.* **30,** 67–112.

Jugo P. J., Candela P. A., and Piccoli P. M. (1999) Magmatic sulfides and Au : Cu ratios in porphyry deposits: An experimental study of copper and gold partitioning at 850°C, 100 MPa in a haplogranitic melt-pyrrhotite-intermediate solid solution-gold metal assemblage, at gas saturation. *Lithos* **46,** 573–589.

Kohn S. C., Dupree R., and Smith M. E. (1989) A multinuclear magnetic resonance study of the structure of hydrous albite glasses. *Geochim. Cosmochim. Acta* **53,** 2925–2935.

Loucks R. R. and Mavrogenes J. A. (1999) Gold solubility in supercritcal hydrothermal brines measured in synthetic fluid inclusions. *Science* **284,** 2159–2163.

McMahon G., Cabri L. J., Hamed A., Hervig R. L., and Williams P. (2000) Trace analyses of Pt and Au using primary ion beams of Cs+ and K+ — A comparative study. In *Secondary Ion Mass Spectrometry, SIMS XII* (eds. A. Benninghoven et al.), pp. 131–134, Elsevier, Amsterdam.

McMillan P. F. (1994) Water solubility and speciation models. In *Volatiles in Magmas* (eds. M. R. Carroll and J. R. Holloway), *Mineralogical Society of America* **30,** 131–152.

Pan P. and Wood S. A. (1991) Gold-chloride complexes in very acidic aqueous solutions and at temperatures 25–300°C: A laser Raman spectroscopic study. *Geochim. Cosmochim. Acta* **55,** 2365–2371.

Piccoli P. M., Candela P. A., and Williams T. J. (1999) Estimation of aqueous HCl and Cl concentrations in felsic systems. *Lithos* **46,** 591–604.

Ratajeski K. and Campbell A. R. (1994) Distribution of fluid inclusions

in igneous quartz of the Capitan Pluton, New Mexico, USA. *Geochim. Cosmochim. Acta* **58,** 1161–1174.

Renders P. J. and Seward T. M. (1989) The stability of hydrosulphido- and sulphido-complexes of Au(I) and Ag(I) at 25°C. *Geochim. Cosmochim. Acta* **53,** 245–253.

Reyf F. G. (1997) Direct evolution of W-rich brines from crystallizing melt within the Mariktikan granite pluton, west Transbaikalia. *Miner. Deposita* **32,** 475–490.

Richards J. P. and Kerrich R. (1993) The Porgera gold mine, Papua New Guinea: Magmatic hydrothermal to epithermal evolution of an alkalic-type precious metal deposit. *Econ. Geol.* **88,** 1017–1052.

Richards J. P. and Ledlie L. D. (1993) Alkalic intrusive rocks associated with the Mount Kare gold deposit Papua New Guinea: Comparison with the Porgera Intrusive Complex. *Econ. Geol.* **88,** 755–781.

Richards J. P., McCulloch M. T., Chappell B. W., and Kerrich R. (1991) Sources of metal in the Porgera gold deposit, Papua, New Guinea: Evidence from alteration, isotope, and noble metal geochemistry. *Geochim. Cosmochim. Acta* **55,** 565–580.

Shand S. J. (1951) *Eruptive Rocks; Their Genesis, Composition, Classification, and Their Relation to Ore-Deposits, with a Chapter on Meteorites*, Fourth Edition. New York, Hafner Pub. Co.

Sillitoe R. H. (1979) Some thoughts on gold-rich porphyry copper deposits. *Mineral. Deposita* **14,** 161–174.

Sillitoe R. H. (1989) Gold deposits in western Pacific island arcs: The magmatic connection. *Econ. Geol. Monograph* **6,** 274–291.

Singer D. A. (1995) World class base and precious metal deposits — A quantitative analysis. *Econ. Geol.* **90,** 88–104.

Sourirajan S. and Kennedy G. C. (1962) The system NaCl-H_2O at elevated temperatures and pressures. *Am. J. Sci.* **260,** 115–141.

Sterner S. M., Chou I-M., Downs R. T., and Pitzer K. S. (1992) Phase relations in the system NaCl-KCl-H_2O: V. Thermodynamic-*PTX* analysis of solid-liquid equilibria at high temperatures and pressures. *Geochim. Cosmochim. Acta* **56,** 2295–2309.

Stolper E. M. (1982) The speciation of water in silicate melts. *Geochim. Cosmochim. Acta* **46,** 2295–2309.

Tossell J. A. (1996) The speciation of gold in aqueous solution: A theoretical study. *Geochim. Cosmochim. Acta* **60,** 17–29.

Ulrich T., Günther D., and Heinrich C. A. (1999) Gold concentrations of magmatic brines and the metal budget of porphyry copper deposits. *Nature* **399,** 676–679.

Williams T. J., Candela P. A., and Piccoli P. M. (1997) Hydrogen-alkali exchange between silicate melts and two-phase aqueous mixtures: An experimental investigation. *Contrib. Mineral. Petr.* **128,** 114–126.

Zotov A. V., Kudrin A. V., Levin K. A., Shikina N. D., and Var'yash L. N. (1994) Experimental studies of the solubility and complexing of selected ore elements (Au, Ag, Cu, Mo, As, Sb, Hg) in aqueous solutions. In *Fluids in the Crust: Equilibrium and Transport Properties* (eds. K. I. Shmulovich et al.), pp. 95–137, Chapman & Hall, London.